NANOSYSTEMS: PHYSICS, CHEMISTRY, MATHEMATICS, 2016, 7 (1), P. 37–43

Electrical properties of carbon nanotubes / WS_2 nanotubes (nanoparticles) hybrid films

V. K. Ksenevich[1], N. I. Gorbachuk[1], Ho Viet[1], M. V. Shuba[2], P. P. Kuzhir[2], S. A. Maksimenko[2], A. G. Paddubskaya[3], G. Valusis[3], A. D. Wieck[4], A. Zak[5], R. Tenne[6]

[1]Department of Physics, Belarusian State University, Minsk, Belarus
[2]Research Institute for Nuclear Problems, Belarusian State University, Minsk, Belarus
[3]Center for Physical Sciences and Technology, Vilnius, Lithuania
[4]Department of Physics and Astronomy, Bochum Ruhr-University, Bochum, Germany
[5]Department of Sciences, Holon Institute of Technology, Holon, Israel
[6]Department of Materials and Interfaces, Weizmann Institute of Science, Rehovot, Israel

ksenevich@bsu.by

PACS 73.63.Fg **DOI 10.17586/2220-8054-2016-7-1-37-43**

DC and AC electrical properties of hybrid films, consisting of carbon nanotubes and tungsten disulfide nanotubes (and fullerene like nanoparticles) were studied within the 2 – 300 K temperature range and over the 20 Hz – 1 MHz frequency range. The temperature dependences of the resistance $R(T)$ exhibit behavior typical for the fluctuation-induced tunneling model in the intermediate temperature range. Analysis of the dependences of real and imaginary components of the impedance on the frequency ($Z'(f)$ and $Z''(f)$) demonstrates the rising role of the contact barriers between carbon nanotubes inside hybrid films, consisting of the carbon nanotubes and inorganic tungsten disulfide nanotubes as the temperature was decreased. The active component of the impedance was found to prevail in the AC electrical properties of the hybrid films, consisting of multi-wall carbon nanotubes and WS_2 nanoparticles over the entire available temperature range.

Keywords: carbon nanotubes, inorganic nanotubes, tungsten disulfide, impedance, electrical properties.

Received: 20 November 2015

1. Introduction

The electrical and electromagnetic properties of carbon nanotubes (CNT) and tungsten disulfide nanostructures of different morphology (tubular and semi-spherical) are of particular interest, due to the number of their possible applications. Different types of CNT-based structures can be utilized for manufacturing of various integrated-circuit elements and electromagnetic devices, for example, transmission lines [1], interconnects [2], and nanoantennas [3,4]. Undoped WS_2 nanotubes exhibit semiconductor properties with a well-defined band gap and with direct or indirect transition, depending on chirality [5]. High quality field-effect transistors based on WS_2 nanotubes were recently demonstrated [6].

Hybrid materials based on carbon and inorganic nanostructures attracted a lot of interest, due to their unique electrical, mechanical, optical and thermal properties [7]. The multifunctionality of hybrid nanocomposites provides possibility for a number of applications of these materials, including gas sensors, chemical sensors, supercapacitors, batteries and photovoltaic elements [8].

We assume that new class of hybrid materials consisting of organic (carbon nanotubes) and inorganic components (WS_2 nanotubes (NT) or WS_2 nanoparticles (NP)), which are commercially available, can be used for fabricating media with electrical properties and electromagnetic parameters that can be varied over a wide range. In this paper, we have focused our efforts on characterization of low frequency AC and DC electrical properties of such hybrid films.

2. Experimental details

Both single-wall carbon nanotubes (SWCNT) and multi-wall carbon nanotubes (MWCNT) were used as organic components for the fabrication of hybrid films. Commercially available HipCO SWCNT (with diameter of 0.8 – 1.2 nm and length in the range 100 nm – 1 μm) and CVD-produced MWCNT (with diameter of 30 – 50 nm and length in the range 0.5 nm – 200 μm) were utilized for hybrid films fabrication. WS_2 nanotubes were grown in the large-scale fluidized-bed reactor. A detailed description of the growth mechanism was given in [9]. Careful parameterization of the conditions within the reactor allowed the scaling-up of nanotube synthesis to the current level of 150 g/day of pure nanotubes. The synthesized nanotube powder is rather fluffy and can easily be dispersed in different solvents and polymer blends and do not require an additional deagglomeration process. The majority of the WS_2 nanotubes are 1 – 30 μm in length and 20 – 180 nm in diameter. According to the HRTEM analysis tungsten disulfide nanotubes reveal highly crystalline order as one can see also from Fig. 1a. Inorganic fullerene-like WS_2 nanoparticles of 50 – 150 nm in diameter were synthesized by a high temperature (850 °C) reaction using H_2S gas and strongly reducing conditions in a fluidized bed reactor.

SWCNT/WS_2-NT and MWCNT/WS_2-NP hybrid films were produced on a cellulose acetate membrane filter (Millipore, 0.22 μm pore size) via a filtration process. In a typical procedure, 0.2 mg of each type of CNTs was dispersed into 1 wt% SDS aqueous solution by ultrasonication for 1 h at 44 kHz. In order to remove the remaining CNT agglomerates, thick CNT bundles and catalytic particles, the prepared suspension was subjected to centrifugation for 10 min at an acceleration of 12000 g. The surfactant was washed away with distilled water. CNT and inorganic WS_2 nanotubes (fullerenes) were mixed in the filtration cell. Typical SEM image of SWCNT/WS_2-NT hybrid film is shown in Fig. 1b. TEM micrograph of a typical WS_2NP with fullerene-like structure is shown in Fig. 1c. This nanoparticle consists of some 25 concentric and closed layers of WS_2, but is not free of point defects, especially at points of acute curvature angles. Typical SEM image of SWCNT/WS_2-NP hybrid film is shown in Fig. 1d. In order to determine influence of inorganic nanotubes (nanoparticles) on the electrical properties of hybrid films, pure SWCNT and MWCNT films were fabricated using the same filtration procedure.

After filtration, the films were transferred onto insulating Al_2O_3 substrates for further electrical characterization. Electrical contacts to the films were made by Ag paint. Measurements of the temperature dependences of resistance $R(T)$ were carried out in the temperature range 2 – 300 K using close-cycled refrigerator CFHF of Cryogenics Ltd.

Characterization of AC electrical properties was done by means of impedance spectroscopy using a LCR meter (Agilent 4284A). Measurements of the complex impedance $Z = Z' + iZ''$ of the hybrid films were performed over frequencies ranging from 20 Hz to 1 MHz at 4.2, 77 and 300 K. The amplitude of the sinusoidal signal was 40 mV. DC bias voltage in the range 0 – 5 V was simultaneously applied to the examined samples. Modeling of the experimental results by equivalent circuits was done using an EIS Spectrum Analyzer 1.0 program.

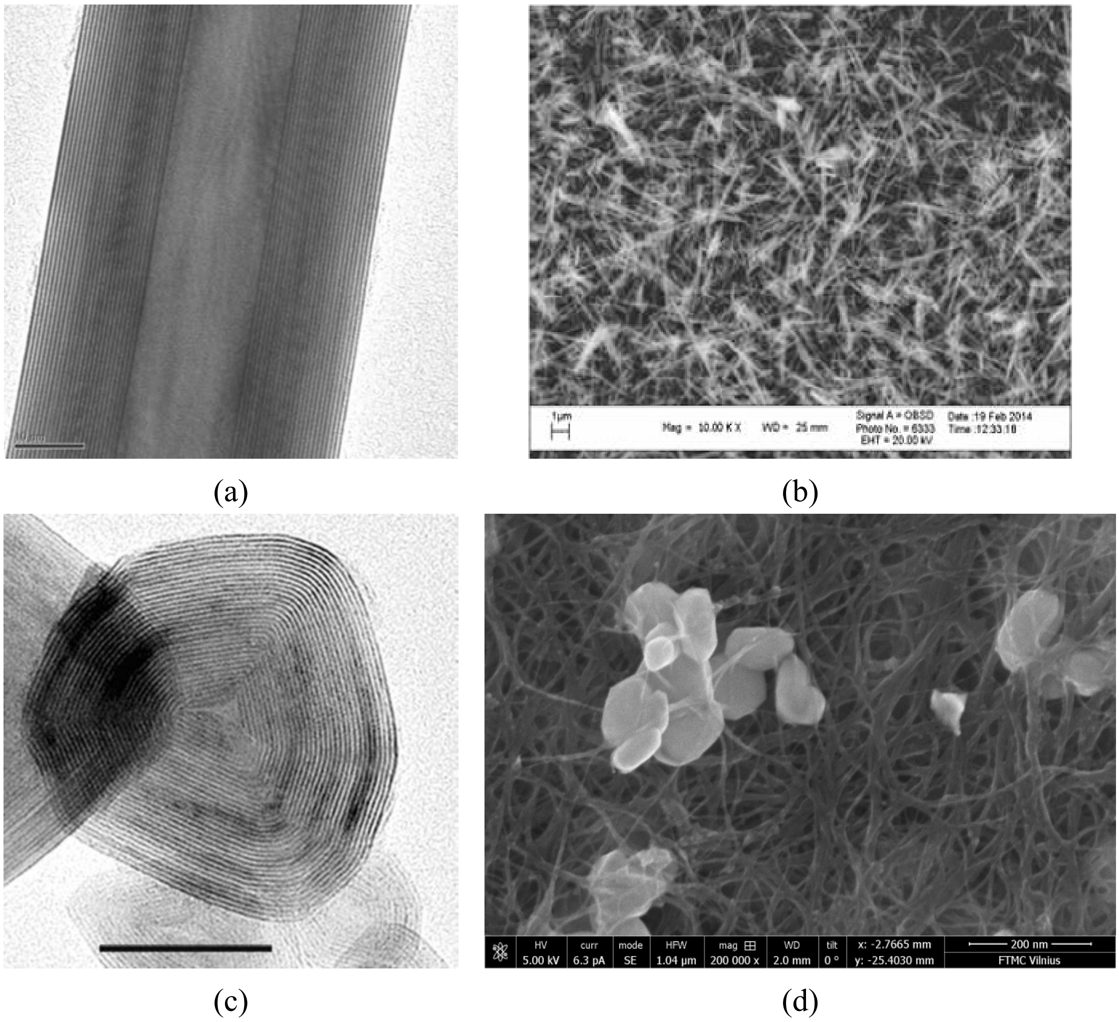

FIG. 1. (a) HRTEM image of WS_2 nanotube, scale bar is 10 nm; (b) SEM image of SWCNT/WS_2-NT hybrid film, scale bar is 1 μm; (c) HRTEM image of a typical fullerene-like nanoparticle of WS_2, scale bar is 20 nm; (d) SEM image of MWCNT/WS_2-NP hybrid film, scale bar is 200 nm

3. Experimental results and discussion

3.1. DC conductivity

Temperature dependences of the resistance $R(T)$ of SWCNT films and SWCNT/WS_2-NT hybrid films which have approximately the same geometrical sizes (width, length and thickness of the films) are presented in Fig. 2. $R(T)$ dependences of MWCNT films and MWCNT/WS_2-NP hybrid films are shown in Fig. 3. Both types of the samples (pure CNT films and hybrid films) have similar $R(T)$ dependences, characterized by negative temperature coefficient of the resistance ($dR/dT < 0$) over the entire temperature range (2 – 300 K). As one can see from Figs. 2 and 3, hybrid films have higher resistance values in comparison to pure SWCNT and MWCNT films. The difference in the conductivities of pure CNT films and hybrid samples increased as the temperature decreased. In the intermediate temperature range, it was found that the temperature dependences of the resistance $R(T)$ can be approximated by the equation proposed within the framework of inherent for disordered systems fluctuation-induced tunneling model [10]:

$$R = R_0 \exp(T_1/T + T_0), \tag{1}$$

where T_1, according to [10], is the temperature below which conduction is dominated by the charge carrier tunneling through the barrier and T_0 is the temperature above which fluctuation effects become significant. This model can be applied for fitting of the electrical properties of different types of disordered systems (including carbon nanotubes arrays [11] and CNT based polymer composites [12]) in which large in atomic scale highly conductive regions divided by small insulating barriers.

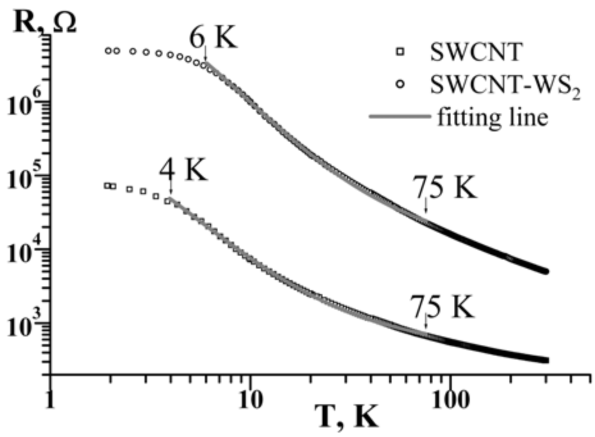

FIG. 2. The temperature dependence of the resistance $R(T)$ (in $\log - \log$ scale) of SWCNT film and SWCNT/WS_2-NT hybrid film. Solid lines are fitted results from Eq. (1)

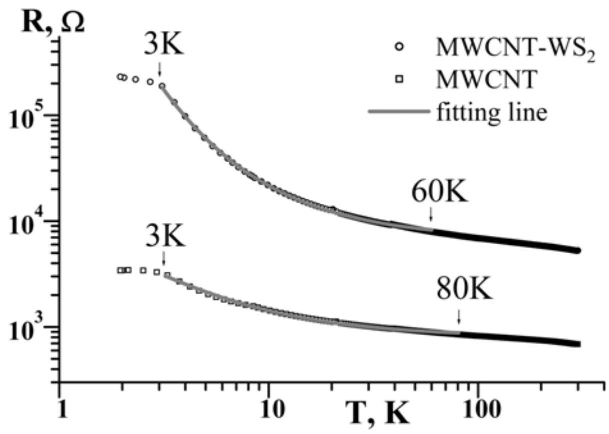

FIG. 3. The temperature dependence of the resistance $R(T)$ (in $\log - \log$ scale) of MWCNT film and MWCNT/WS_2-NP hybrid film. Solid lines are fitted results from Eq. (1)

The low temperature saturation of the resistance can be explained by the tendency to saturate the dephasing time of the charge carriers inside an individual CNT observed in weakly disordered systems [13]. In order to approximate the experimental data over the entire temperature range, a more complicated analysis is required, which takes into account strong and/or weak localization effects.

3.2. AC conductivity

Impedance spectroscopy is a powerful tool for characterizating different types of disordered structures [14], including nanocomposites and arrays of carbon nanotubes. Measurements of the relationships between the real and imaginary components of the impedance and the frequency, $Z'(f)$ and $Z''(f)$, along with the following of theoretical modeling of experimental results, provides the possibility for dividing the contribution from the nanotubes themselves and the contact barriers between them into the total impedance of the CNT assemblies.

It was found that over the entire temperature range, 4.2 – 300 K, both the pure SWCNT and MWCNT films demonstrate properties inherent for the structures with a prevailing active part of the complex impedance. Incorporation of tungsten disulfide nanotubes into the SWCNT films and tungsten disulfide nanoparticles into the MWCNT films exhibited different influences on the AC electrical properties of hybrid films. Analysis of the $Z'(f)$ and $Z''(f)$ dependences for the SWCNT/WS_2-NT hybrid films clearly demonstrate the increasingly important role of the reactive part of the complex impedance as the temperature decreases. It was found that for all measurement temperatures (4.2, 77 and 300 K) complex impedance of the SWCNT/WS_2-NT hybrid films can be modeled using an equivalent circuit consisting of the following elements connected in series and parallel: resistance R_1, capacitance C, resistance R_2 and constant phase element *CPE*. Impedance diagram of the SWCNT/WS_2-NT hybrid films reconstructed from $Z'(f)$ and $Z''(f)$ dependences measured at $T = 4.2$ K is presented in Fig. 4. Due to the low conductivity of WS_2 nanotubes in comparison to the SWCNTs, we assume that in the equivalent circuit (shown in the inset to Fig. 4), calculated for hybrid film, the resistance R_1 and the capacitance C correspond to the average values of resistance and capacitance for the carbon nanotubes. On the other hand, the resistance R_2 simulates the Ohmic resistance of contact regions between the SWCNTs. The element *CPE* takes into account the spread in values of the resistance and capacitance of the inter-nanotube contact barriers [14]. The admittance of the CPE is defined as:

$$Y_{CPE} = A_0(i\omega)^\alpha = A_0[\cos(\pi/2\alpha) + i\sin(\pi/2\alpha)], \tag{2}$$

where A_0 is the coefficient with the dimensionality depending on the α value. In the case of $\alpha = 1$, the coefficient A_0 has the dimensionality of capacitance, while in the case $\alpha = 0$, the coefficient A_0 has the dimensionality of resistance. In the intermediate case, the dimensionality of A_0 can be considered as $\Omega^{-1} \cdot s^\alpha$ [15].

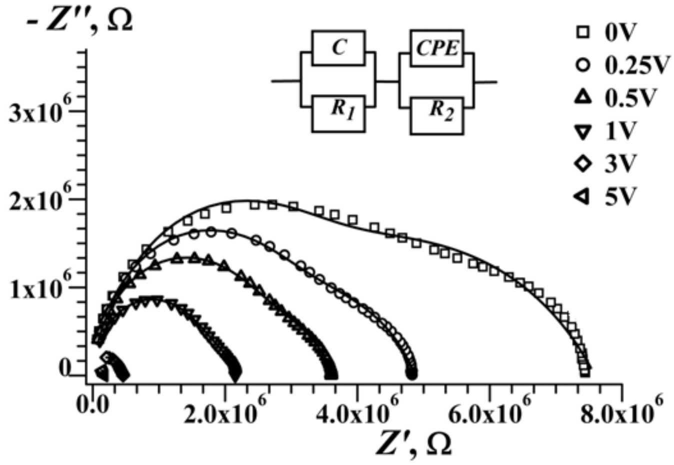

FIG. 4. Impedance diagrams of SWCNT/WS_2-NT hybrid films measured at temperature $T = 4.2$ K and at different value of applied DC voltage. Lines show the approximation of the experimental data by an equivalent circuit, presented in the inset

Unlike the SWCNT films and SWCNT/WS_2-NT hybrid films, the imaginary components of the impedance for both types of MWCNT samples (pure CNT films and hybrid films) were very low in comparison with the active parts of their impedance, even at $T = 4.2$ K and without applied DC bias voltage. The maximum value for the phase shift between voltage and current of about -10 $^\circ$ at 1 MHz was observed for MWCNT/WS_2-NP hybrid films at $T = 4.2$ K and at $U_b = 0$ V. This fact indicates that the electrical contacts between individual MWCNT inside pure and hybrid films were good, even in the low temperature range. Thus, the influence of WS_2 nanoparticles incorporation into MWCNT films on the frequency dependence of the impedance is less important in comparison to the case when the WS_2 nanotubes were embedded into the SWCNT films. This can be attributed to a geometrical factor. WS_2 nanotubes and SWCNT are characterized by large difference in sizes (20 – 180 nm *vs* 0.8 – 1.2 nm in diameter and 1 – 30 μm *vs* 100 nm – 1 μm in length, for WS_2-NT and SWCNT, respectively). Therefore incorporation of poorly conducting WS_2 nanotubes into the matrix consisting of highly conductive SWCNT strongly increases the role of the contact resistance between separate single-wall carbon nanotubes inside the film. Conversely, embedding of the spherical WS_2 nanoparticles with diameter in the range 50 – 150 nm into the film consisting of MWCNT (with diameter of 30 – 50 nm and length in the range 0.5 nm – 200 μm) does not strongly affect the AC conductivity of films.

One of the most interesting features of the AC electrical properties of the examined samples is the existence of a highly reproducible positive value for the imaginary component of impedance observed at $T = 4.2$ K for SWCNT films, MWCNT films and MWCNT/WS_2-NP hybrids, as the DC bias voltage was applied. These positive Z'' values (corresponding to the negative part of $-Z''(f)$ plots) are clearly seen in Figs. 5 and 6 and can be explained by the increased role of kinetic inductance for individual carbon nanotubes [16] as the temperature decreased and DC voltage was applied. This effect was not observed for SWCNT/WS_2-NT hybrid films due to the high value of negative (capacitive) part of reactive impedance at low temperatures.

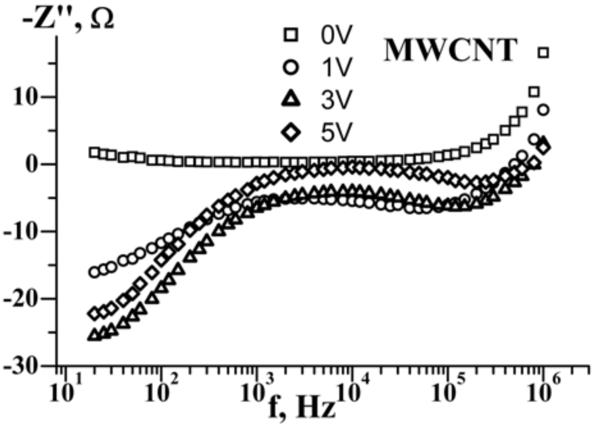

FIG. 5. Frequency dependence of the imaginary component of the impedance $-Z''(f)$ of MWCNT film measured at $T = 4.2$ K

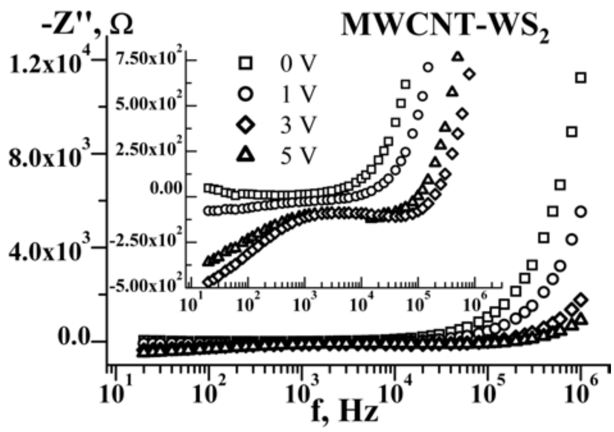

FIG. 6. Frequency dependence of the imaginary component $-Z''(f)$ of the impedance of MWCNT/WS_2-NP hybrid films measured at $T = 4.2$ K. Low-ohmic part of $-Z''(f)$ value is shown in the inset

It should be noted, that due to the low value of reactive part of the impedance Z'' in comparison with the active component Z', the modeling of experimental results for MWCNT films and MWCNT/WS_2-NP hybrid films by reasonable equivalent circuits was impossible.

4. Conclusion

Investigation of the AC and DC electrical properties of the nanocomposite materials consisting of carbon nanotubes and inorganic tungsten disulfide nanotubes (nanoparticles) provided evidence for the successful processing of electrically conductive hybrid films using the filtration method. Incorporation of WS_2 nanotubes and nanoparticles into the carbon nanotube arrays was found to reduce strongly the electrical conductivity of fabricated hybrids. Further research will be focused on assessing the possibility of tuning the conductivity and dielectric constant of composites over a wide range by varying the percentage ratio of the carbon and inorganic components.

Acknowledgments

This work was supported by Belarusian National Research Program "Nanomaterials and Nanotechnologies" (grant No. 2.2.02), by FP7 project PIRSES-2012-318617 FAEMCAR and FP7-316633 POCAONTAS, Tomsk State University Competitiveness Improvement Program, and Federal Focus program of Ministry of Education and Science of Russian Federation # 14.577.21.0006 (project ID RFMEFI57714X0006). We are thankful for Prof. Stefano Bellucci (LNF INFN Italy) for fruitful discussions, valuable comments, and providing us with MWCNT samples.

References

[1] Slepyan G.Ya., Maksimenko S.A., et al. Electrodynamics of carbon nanotubes: Dynamic conductivity, impedance boundary conditions, and surface wave propagation. *Phys. Rev. B*, 1999, **60** (24), P. 17136–17149.

[2] Rybczynski J., Kempa K., et al. Subwavelength waveguide for visible light. *Appl. Phys. Lett.*, 2007, **90**, 021104 (1–3).

[3] Hanson G.W. Fundamental transmitting properties of carbon nanotube antennas. *IEEE Trans. Antennas Propag.*, 2005, **53** (11), P. 3426–3435.

[4] Slepyan G.Ya., Shuba M.V., Maksimenko S.A., Lakhtakia A. Theory of optical scattering by achiral carbon nanotubes and their potential as optical nanoantennas. *Phys. Rev. B*, 2006, **73** (19), 195416 (1–11).

[5] Seifert G., Terrones H., et al. On the electronic structure of WS_2 nanotubes. *Solid State Commun.*, 2000, **114** (5), P. 245–248.

[6] Levi R., Bitton O., et al. Field-Effect Transistors Based on WS_2 Nanotubes with High Current-Carrying Capacity. *Nano Lett.*, 2013, **13** (8), P. 3736–3741.

[7] Naffakh M., Diez-Pascual A.M., Gomez-Fatou M.A. New hybrid nanocomposites containing carbon nanotubes, inorganic fullerene-like WS_2 nanoparticles and poly(ether ether ketone) (PEEK). *J. Mater. Chem.*, 2011, **21** (20), P. 7425–7433.

[8] Eder D. Carbon Nanotube – Inorganic Hybrids. *Chem. Rev.*, 2010, **110** (3), P. 1348–1385.

[9] Zak A., Sallacan-Ecker L., et al. Insight into the Growth Mechanism of WS_2 Nanotubes in the Scaled-Up Fluidized-Bed Reactor. *NANO*, 2009, **04** (02), P. 91–98.

[10] Sheng P. Fluctuation-Induced Tunneling Conduction in Disordered Materials. *Phys. Rev. B*, 1980, **21** (6), P. 2180–2195.

[11] Ksenevich V.K., Dauzhenka T.A., et al. Electrical transport in carbon nanotube coatings of silica fibers. *Phys. Status Solidi C*, 2009, **6** (12), P. 2798–2800.

[12] Kuzhir P., Ksenevich V.K., et al. CNT based epoxy resin composites for conductive applications. *Nanosci. Nanotechnol. Lett.*, 2011, **3** (6), P. 889–894.

[13] Gershenson M.E. Low-Temperature Dephasing in Disordered Conductors: Experimental Aspects. *Annalen der Physik (Leipzig)*, 1999, **8** (7–9), P. 559–568.

[14] Barsoukov E., Macdonald J.R. (Eds.) *Impedance Spectroscopy. Theory, Experiment, and Applications*. Wiley, Hoboken, 2005, 616 p.

[15] Sluyters-Rehbach M. Impedances of electrochemical systems: Terminology, nomenclature and representation – Part I: Cells with metal electrodes and liquid solutions. *Pure and Appl. Chem.*, 1994, **66** (9), P. 1831–1891.

[16] Burke P.J. An RF Circuit Model for Carbon Nanotubes. *IEEE Trans. Nanotechnol.*, 2003, **2** (1), P. 55–58.